Physiological Ligands ADP and P_i Modulate the Degree of Intrinsic Coupling in the ATP Synthase of the Photosynthetic Bacterium *Rhodobacter capsulatus*†

Paola Turina,* Donatella Giovannini, Francesca Gubellini, and B. Andrea Melandri

Department of Biology, Laboratory of Biochemistry and Biophysics, University of Bologna, Via Irnerio 42, 40126 Bologna, Italy

Received May 20, 2004; Revised Manuscript Received June 25, 2004

ABSTRACT: The proton-pumping and the ATP hydrolysis activities of the ATP synthase of *Rhodobacter capsulatus* have been compared as a function of the ADP and P_i concentrations. The proton pumping was measured either with the transmembrane pH difference probe, 9-amino-6-chloro-2-methoxyacridine, or with the transmembrane electric potential difference probe, bis(3-propyl-5-oxoisoxazol-4-yl)pentamethine oxonol, obtaining consistent results. The comparison indicates that an intrinsic uncoupling of ATP synthase is induced when the concentration of either ligand is decreased. The half-maximal effect was found in the submicromolar range for ADP and at about 70 μM for P_i. It is proposed that a switch from a partially uncoupled state of ATP synthase to the coupled state is induced by the simultaneous binding of ADP and P_i.

Membrane-bound F_0F_1-ATPases[1] or ATP synthases catalyze ATP synthesis in bacteria, chloroplasts, and mitochondria at the expense of an electrochemical potential gradient of protons (or Na^+ ions in some species). They can usually work also in the ATP hydrolysis direction, by building up a proton gradient. Their membrane-embedded hydrophobic F_0 sector is involved in proton translocation across the membrane, and their hydrophilic F_1 sector contains the catalytic sites (*1*−*4*). Since the first crystal structure of the mitochondrial F_1 was reported (*5*), high-resolution structural information for the soluble part has continued to appear, although a high-resolution structure of the holo complex is still lacking.

In the currently accepted view of the rotational mechanism of catalysis, the γ- and ϵ-subunit in F_1 and the *c*-subunit ring in F_0 constitute the rotor, which in the hydrolysis direction, is driven by ATP to rotate against subunit *a* in F_0 and, in the synthesis direction, is driven by the proton flow to rotate against the $\alpha_3\beta_3$-subunit barrel in F_1.

In several studies, the high efficiency of energy transduction within this remarkable "rotary enzyme" has been emphasized (*3*, *6*, *7*). On the other hand, plenty of studies have appeared testifying about the occurrence of uncoupling between the ATP hydrolysis reaction and the proton transport device, either induced by mutations or chemical modification (*8*−*9* and references therein, *10*) or by nonphysiological ligands such as Ca^{2+} (*11*, *12*) and sulfite (*13*).

To our knowledge, no experimental evidence has been presented so far about uncoupling in the native, wild-type enzyme. The H^+/ATP ratio has generally been considered a fixed parameter (but see ref *14* and references therein, *15*, *16*). On the other hand, the phenomenon of high proton conductance through F_0 at low ADP or P_i concentrations, well-known in chloroplasts (*17*−*20*) and photosynthetic bacteria (*21*), has been considered as a case of intrinsic uncoupling. No evidence has been presented so far indicating the occurrence of this uncoupling while the enzyme is actually catalyzing ATP synthesis or hydrolysis.

In this paper, we show that an intrinsically uncoupled state of the unmodified, wild-type ATP synthase can be detected during its activity in the ATP hydrolysis direction, provided that the concentration of either ADP or P_i is maintained at a low level.

MATERIALS AND METHODS

Bacterial Strains, Growth Conditions, and Membrane Preparations. A pseudo-wild-type strain of *Rhodobacter (Rb.) capsulatus* has been used originating from strain B100, which is wild-type strain B10 cured of phages. The strain, described in ref *22*, carries a Kanamycin resistance cassette in place of the chromosomal copy of the *atp1* operon (containing the F_1 genes) and harbors a plasmid carrying a copy of this operon together with a tetracycline resistance cassette. The cells were grown photoheterotrophically on a synthetic medium containing malate as a carbon source (*23*); kanamycin and tetracycline were added at 25 and 2 μg/mL, respectively. Cultures were illuminated by two opposite panels each carrying nine 100 W incandescent light bulbs;

† This work has been supported by the Grant PRIN/2003 "Bioenergetica: Genomica funzionale, meccanismi molecolari ed aspetti fisiopatologici" from the Italian Ministery for Education of University and Research (MIUR).

* To whom correspondence should be addressed: Laboratory of Biochemistry and Biophysics, Department of Biology, University of Bologna, Via Irnerio, 42, I-40126 Bologna, Italy. Telephone: ++39 (051) 2091322. Fax: ++39 (051) 242576. E-mail: turina@alma.unibo.it. Website: http://www.biologia.unibo.it.

[1] Abbreviations: F_0, transmembrane sector of the ATP synthase; F_1, hydrophilic, extrinsic sector of the ATP synthase; Bchl, bacteriochlorophyll; ACMA, 9-amino-6-chloro-2-methoxyacridine; tricine, *N*-[2-hydroxy-1,1-bis(hydroxymethyl)ethyl]glycine; oxonol VI, bis(3-propyl-5-oxoisoxazol-4-yl)pentamethine oxonol; $\Delta\varphi$, bulk-to-bulk transmembrane electrical potential difference; PK, pyruvate kinase; Phenol Red, 4,4′-(3*H*-2,1-benzoxathiol-3-ylidene)bisphenol,*S*,*S*-dioxide; LDH, lactate dehydrogenase; PNP, purine nucleoside phosphorylase; MESG, 2-amino-6-mercapto-7-methylpurine riboside; $\Delta\tilde{\mu}_{H^+}$, transmembrane difference of electrochemical potential of protons; ΔpH, transmembrane difference of pH.

10.1021/bi048975+ CCC: $27.50
Published on Web 08/06/2004

excessive warming was prevented by water cooling. Cells were harvested at $OD_{600} = 1.2-1.4$. Intracytoplasmic membranes (chromatophores) were prepared by the method given in ref *23*, resuspended in 50 mM glycyl-glycine/NaOH and 5 mM $MgCl_2$ at pH 7.5, rapidly frozen as small droplets in liquid nitrogen, and stored at −80 °C. The bacteriochlorophyll (Bchl) concentration was measured in an acetone−methanol extract (*24*).

9-Amino-6-chloro-2-methoxyacridine (ACMA) Assay. ACMA fluorescence quenching assays were carried out in a Jasco FP 500 spectrofluorometer (wavelength 412 and 482 nm for excitation and emission, respectively) at 34 °C. Chromatophores were suspended to 1 μM Bchl in the following buffer: 1 mM *N*-[2-hydroxy-1,1-bis(hydroxymethyl)ethyl]glycine (tricine), 20 mM succinic acid, 50 mM KCl, 2.5 mM $MgCl_2$, NaOH at pH 8.0, and 0.1 μM valinomycin to minimize $\Delta\varphi$; the inhibitors of the electron transport chain antimycin (5 μM) and myxothiazol (10 μM); and ACMA was added to 0.7 μM. This chromatophores suspension is indicated as the "ACMA mixture". Antimycin and myxothiazol prevented the actinic effect of the excitation light, because no ACMA quenching could be detected during the exposure for 5 min to the excitation beam, but they did not affect ATP hydrolysis rates. The buffer capacity was kept low to measure ATP hydrolysis with 4,4′-(3*H*-2,1-benzoxathiol-3-ylidene)bisphenol,*S*,*S*-dioxide (Phenol Red) under the same buffer conditions. Prior to each measurement, the sample pH was adjusted to 8.0 with NaOH.

Oxonol Assay. Bis(3-propyl-5-oxoisoxazol-4-yl)pentamethine oxonol (oxonol VI) absorption changes were recorded as a function of time in a Jasco V-550 spectrophotometer in dual-wavelength mode (625−587 nm) at 23 °C. Chromatophores were suspended to 5 or 7.5 μM Bchl in the following buffer: 5 mM tricine, 1 mM succinic acid, 50 mM K-acetate, 2.5 mM Mg-acetate, NaOH at pH 8.0, 2 μM nigericine to minimize the transmembrane pH difference (ΔpH), 10 nM valinomycin, 5 μM antimycin, and 10 μM myxothiazol; oxonol VI was added to 3 μM. This chromatophores suspension is indicated as the "oxonol mixture". In the absence of added ATP, no change of the oxonol VI signal was detected by exposure to the measuring beam, indicating that its low intensity and the presence of the inhibitors antimycin and myxothiazol prevented the buildup of any significant $\Delta\varphi$. Even in these assays, the buffer capacity was kept low to measure ATP hydrolysis with Phenol Red under the same buffer conditions. Prior to each measurement, the sample pH was adjusted to 8.0 with NaOH.

ATP Hydrolysis. ATP hydrolysis was measured under experimental conditions as close as possible to those used in the ACMA and oxonol assays. In the absence of the pyruvate kinase (PK) or P_i trap, the ATP hydrolysis was measured by detecting the stoichiometric protons released upon ATP hydrolysis with the colorimetric pH indicator Phenol Red. The reaction temperature and assay mixtures were the same as those used in the ACMA or oxonol assays, except that 100 μM Phenol Red was present and no ACMA or oxonol VI was added. The pH changes of the suspension were followed as a function of time by the absorbance changes at 625−587 nm and were calibrated after about 300 s of reaction by the 3-fold addition of 15 μM HCl. The overall pH change of the suspension at the end of the measurements was never higher than 0.2 units. The changes of the proton concentration were transformed to changes of the ATP concentration as described (*25*). At pH 8.0, a ratio of chemically released H^+ per hydrolyzed ATP of 0.94 was calculated. When ATP hydrolysis was measured in control samples with the malachite green assay (*26*), the same rates were obtained.

For measurements in the presence of PK, the reaction temperature and ATP hydrolysis mixtures were again the same as used in the ACMA or oxonol assays, including the low buffer concentration, except that lactate dehydrogenase (LDH) (40 units/mL), NADH (0.11 mM), and 2 mM KCN were present and no ACMA or oxonol VI was added. The ADP trap was thus further coupled to NADH oxidation.

In some measurements (see Figure 5A), the EnzCheck Phosphate Assay Kit (Molecular Probes) was used as a detection method and efficient P_i trap. This assay (*27*) is a combination of purine nucleoside phosphorylase (PNP), added at 1 unit/mL, and of the chromogenic nucleoside 2-amino-6-mercapto-7-methylpurine riboside (MESG), added at 0.2 mM. To measure the ATP hydrolysis activity, the conversion of MESG to its products upon phosphorylation by PNP was followed at 360 nm as a function of time (see Figure 5C). The hydrolysis assays differed from the $\Delta\varphi$ measurements only in that they lacked oxonol VI, and PNP and MESG were present.

Measurement of PK Activity. The activity of PK under the experimental conditions of the present paper was measured both in the ACMA mixture at 34 °C and in the oxonol mixture at 23 °C. The mixtures lacked chromatophores and were supplemented with 1 mM P_i, 2 mM PEP, 2 mM ADP, 0.2 mM NADH, 40 units/mL LDH. The reaction was started in the spectrophotometer by addition of PK (approximately 0.03 units), and the coupled NADH oxidation was recorded at 340 nm.

RESULTS

Vesicles of *Rb. capsulatus* are a well-behaved chemiosmotic system, which has been widely used to investigate functional properties of the involved protein complexes. In particular, the generation of a transmembrane difference of electrochemical potential of protons ($\Delta\tilde{\mu}_{H^+}$) by the photosynthetic electron transport chain and by the ATP synthase has been revealed and investigated by means of several techniques, among which fluorescent acridines as probes of ΔpH (*28*), carotenoid shift (*21*, *29*, *30*), and oxonols as probes of $\Delta\varphi$ (transmembrane electrical potential difference) (*30*). To estimate the proton-translocating activity of the ATP synthase under various conditions, we have used in parallel both the ΔpH probe ACMA and the $\Delta\varphi$ probe oxonol VI.

Figure 1A presents ACMA fluorescence traces obtained upon addition of 100 μM ATP to chromatophores in the presence of PEP and of different amounts of PK. PEP and PK were chosen as a way to modulate the ADP concentration in the assay. Valinomycin and 50 mM K^+ were present to keep the electrical component of $\Delta\tilde{\mu}_{H^+}$ to a negligible level. In the absence of PK (trace a), addition of ATP induced a progressive fluorescence quenching (up to 60% in this case), which is related to a progressive increase of ΔpH. After a few minutes, a stationary state is reached in which the rate of proton translocation from the external to the internal phase is balanced by the rate of passive proton efflux through the

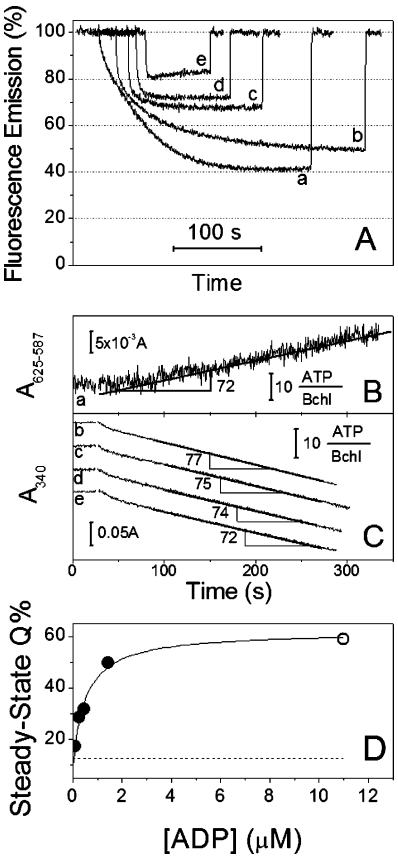

FIGURE 1: ΔpH formation and ATP hydrolysis in the presence of increasing PK. The ACMA mixture (see the Materials and Methods) was supplemented with 1 mM P_i. (A) ΔpH formation. The proton pumping reaction was started in the spectrofluorometer by addition of 100 μM ATP. Traces b−e were obtained in the presence of 1 mM PEP and of increasing amounts of PK: 1.0 (b), 2.9 (c), 4.8 (d), and 14.4 units/mL (e). The 100% fluorescence level was recovered by adding 0.5 μM nigericine. The traces have been translated along the time axis. (B) ATP hydrolysis. ACMA was omitted, and Phenol Red was added to the ACMA mixture. The ATP hydrolysis reaction was started in the spectrophotometer by addition of 100 μM ATP. The number at the slope is the rate of ATP hydrolysis in units of mM ATP M $Bchl^{-1}$ s^{-1}. (C) ATP hydrolysis. The ACMA mixture contained PEP, KCN, LDH, NADH, and no ACMA. The reaction was started in the spectrophotometer by addition of 100 μM ATP. Traces b−e contained increasing amounts of PK as detailed in A. The numbers at the slopes are the rate of ATP hydrolysis in units of mM ATP M $Bchl^{-1}$ s^{-1}. The traces have been translated along the absorbance axis. (D) Relative steady-state fluorescence quenching, *Q*%, from A, were plotted as a function of the ADP concentration in the steady-state condition, estimated from eq 1 (●) or from the P_i released after 3 min (○). The curve is the best fit to the data of the hyperbolic function $P1 + P2x/(P3 + x)$, with best-fit parameters P1 = 13, P2 = 48, and P3 = 0.5 μM.

membrane in the opposite direction, which is proportional to the ΔpH itself. With increasing concentrations of PK (traces b−e), the initial rate of fluorescence quenching was increased but the steady-state level of fluorescence quenching was progressively decreased, indicating a progressively lower level of ΔpH. In each case, the initial fluorescence was recovered by addition of nigericin, which collapsed the ΔpH or, in similar sets of measurements, by the ATP-synthase-specific inhibitor oligomycin (not shown). Similar effects were also seen in the absence of valinomycin, although as expected, with a slower ACMA response, because of the rapid onset of $\Delta\varphi$. Similar measurements were also carried out using different commercial PK preparations, either as glycerol solutions or as ion-free liophylized powder; in each case, results similar to those presented in Figure 1A were obtained for similar PK activities. No effect was observed in the absence of either PEP or PK.

The rates of ATP hydrolysis corresponding to the different conditions of Figure 1A were then measured in parallel assays, in which great care was taken in reproducing as far as possible the experimental conditions of the ACMA fluorescence assays. In the absence of PK, the release of stoichiometric protons because of ATP hydrolysis was measured as a function of time by Phenol Red absorption changes (Figure 1B). The only differences with the ACMA assay were the absence of ACMA itself and the presence of Phenol Red. In the presence of PK, ATP hydrolysis rates were measured by coupling the PK reaction to the LDH reaction and following the NADH absorption changes as a function of time (Figure 1C). In this case, omission of ACMA and addition of LDH, NADH, and KCN were the only differences to the assay compositions of Figure 1A. At the concentration used (2 mM), KCN inhibited any oxidation of NADH through the branched respiratory chain of *Rb. capsulatus* (*31*) and no NADH oxidation could be detected in the absence of ATP. The resulting rates of ATP hydrolysis were in all cases very similar, regardless of the PK concentration. Thus, while the ATP hydrolysis rates were slightly increased or unaffected by increasing PK (parts B and C of Figure 1), the ΔpH extent was progressively decreased (Figure 1A), indicating a progressive intrinsic uncoupling of the ATP synthase by increasing PK concentrations. The initial rapid decrease of the NADH concentration, evident in the traces of Figure 1B, was due to the amount of ADP present in the added ATP, because it also occurred in the absence of chromatophores. The ADP percentage in our ATP solutions, as measured separately with the coupled NADH assay, was 0.7%.

For similar rates of ADP production by the ATP synthase, a higher concentration of PK in the reaction assay will cause a lower ADP concentration in the steady-state condition. At steady-state conditions, the rate of ATP hydrolysis will balance the rate of the PK reaction, i.e.

$$v(\text{ATP hydrolysis}) = v(\text{PK}) = \frac{V_{\text{max}}^{\text{ADP}}[\text{ADP}]_{\text{ss}}}{[\text{ADP}]_{\text{ss}} + K_{\text{M}}^{\text{ADP}}} \quad (1)$$

where V_{max}^{ADP} and K_M^{ADP} are referred to the PK reaction. V_{max}^{ADP} was measured directly (see the Materials and Methods), K_M^{ADP} = 0.3 mM was taken from the literature (*32*), and *v*(ATP hydrolysis) was taken from Figure 1C. The $[ADP]_{ss}$ evaluated in this way should clearly be considered only approximated, because competition of ATP over ADP and other kinetic alterations of the PK activity have not been considered. In Figure 1D, the values of the ACMA fluorescence quenching are plotted as a function of $[ADP]_{ss}$, evaluated on the basis of eq 1 (●), while the highest [ADP] value (○) was evaluated from the kinetics of P_i release. The half-maximal effect was obtained at [ADP] = 0.5 μM.

As mentioned, the proton-translocating activity of the ATP synthase was monitored also with the $\Delta\varphi$-sensitive probe oxonol VI (Figure 2A). In this case, the ΔpH component of $\Delta\tilde{\mu}_{H^+}$ was kept low by the presence of 50 mM K^+ and

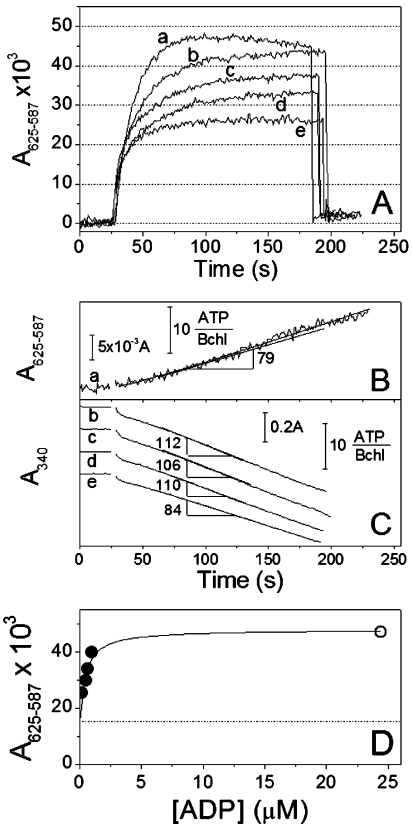

FIGURE 2: $\Delta\varphi$ formation and ATP hydrolysis in the presence of increasing PK. The oxonol mixture (see the Materials and Methods) was 5 μM Bchl and was supplemented with 1 mM P_i. (A) $\Delta\varphi$ formation. The proton pumping reaction was started in the spectrophotometer by addition of 1 mM ATP, and after 150−170 s, 2 μM valinomycin was added to collapse the $\Delta\varphi$. Traces b−e were obtained in the presence of 1 mM PEP and of increasing amounts of PK: 10 (b), 15 (c), 20 (d), and 40 units/mL (e). (B) ATP hydrolysis. Oxonol VI was omitted, and Phenol Red was added to the Oxonol mixture. ATP hydrolysis was started by addition of 1 mM ATP. The curve is the best fit to the data of an arbitrary sigmoid function. A constant slope is observed after an initial lag. The number at the slope is the rate of ATP hydrolysis in units of mM ATP M $Bchl^{-1}$ s^{-1}. (C) ATP hydrolysis. The oxonol mixture contained PEP, KCN, LDH, NADH, and no oxonol VI. The reaction was started in the spectrophotometer by addition of 1 mM ATP. Traces b−e contained increasing amount of PK as detailed in A. The numbers at the slopes are the rate of ATP hydrolysis in units of mM ATP M $Bchl^{-1}$ s^{-1}. (D) Absorption increase after 1 min from A were plotted as a function of the ADP concentration in the steady-state condition, estimated from eq 1 (●) or from the P_i released after 1 min (○). The curve is the best fit to the data of the hyperbolic function $P1 + P2x/(P3 + x)$, with best-fit parameters P1 = 15, P2 = 33, and P3 = 0.5 μM.

nigericin. Very low amounts of valinomycin (10 nM) were also added to these assays to increase the membrane permeability and thereby increase the sensitivity of the static head values of $\Delta\varphi$ to changes in proton-pumping efficiency. Full collapse of $\Delta\varphi$ was induced by increasing the valinomycin concentration to 2 μM. For all traces, an increase in the absorbance at 625−587 nm upon addition of ATP was observed, which is related to a progressive increase of $\Delta\varphi$ from the proton-translocating activity of the ATP synthase. An analogue effect to the one observed in the ACMA assay was also evident in this case: in the absence of PK (trace a), a maximum level of $\Delta\varphi$ was reached, whereas by increasing concentrations of PK the extent of $\Delta\varphi$ was progressively decreased (traces b−e). In the absence of valinomycin traces, similar results were obtained, although the initial rates of absorbance change were higher and steady-state values of the signal were slightly less differentiated, a behavior consistent with the well-documented resistence of steady-state $\Delta\varphi$ to proton-pumping inhibition.

The corresponding ATP hydrolysis rates were measured in parallel as described for parts B and C of Figure 1, under experimental conditions practically identical to those of the oxonol assay. In the absence of PK, the ATP hydrolysis activity was measured with Phenol Red (Figure 2B), and, in the presence of PK, its reaction was coupled to the LDH reaction (Figure 2C). Oxonol VI was omitted in all cases. As expected, the results were very similar to those reported in parts B and C of Figure 1; i.e., the ATP hydrolysis rate did not change significantly at increasing PK concentrations. Again, the ATP hydrolysis results compared to the proton-pumping results indicated a progressive intrinsic uncoupling of the ATP synthase by increasing PK concentrations.

In parallel to Figure 1D, Figure 2D plots the oxonol VI response as a function of the calculated $[ADP]_{ss}$ at different PK concentrations (see eq 1). Also in this case, the half-maximal effect is observed in the submicromolar range.

From the ATP hydrolysis traces of Figure 2B, it can be seen that the kinetics show a slight biphasicity, both in the absence and in the presence of PK. A biphasicity in the rate of ATP hydrolysis has been observed previously in *Rb. capsulatus* (*33*), as well as in other systems, and has been attributed to the release of inhibitory ADP, in coupled vesicles also partly induced by the onset of $\Delta\tilde{\mu}_{H^+}$ (for a general review, see ref *3*). A lower extent of generated $\Delta\tilde{\mu}_{H^+}$ and a lower concentration of ADP in the suspension are possibly the reasons why the traces reported in Figure 1B were not biphasic.

The rates in the presence of PK were about 1.4-fold higher than in its absence, at variance with the ACMA measurements (see Figure 1B compared to Figure 1C). The reasons for this difference were not further investigated but are consistent with the higher concentrations of inhibitory ADP (see below) initially present and then produced in the oxonol assay lacking PK, given the higher ATP (1 mM versus 100 μM) and Bchl (5 μM versus 1 μM) concentrations employed.

The inhibitory effect of ADP on the ATP hydrolysis activity of the ATP synthase is well-known. We have measured the initial rate of ATP hydrolysis with Phenol Red without added PK as a function of the ADP concentration added in the ATP solution under conditions of both ACMA and oxonol assays (not shown); in both cases, the inhibition could be fitted with a hyperbolic function, with half-maximal effects at 30 μM (ACMA) and 83 μM (Oxonol) ADP, with the difference being consistent with the different ATP concentrations in the two assays (0.1 and 1 mM, respectively). The corresponding rates of ACMA quenching and oxonol VI signal change could also be fitted with hyperbolic functions, yielding half-maximal effects at 45 μM (ACMA) and 23 μM (Oxonol) ADP, which were different from those obtained from ATP hydrolysis as expected from the non-linearity of the probes (see the Discussion). We conclude that the ADP-binding site responsible for the uncoupling effects reported here is different from the ADP-binding site responsible for ATP hydrolysis inhibition, because its affinity for ADP appears to be 1−2 orders of magnitude higher.

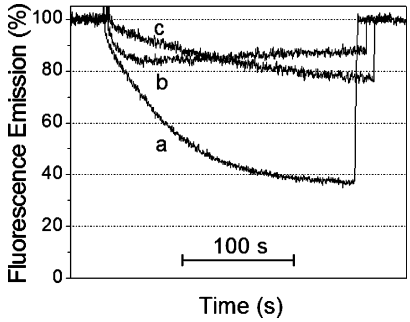

FIGURE 3: ΔpH formation in the absence and presence of added P_i. The ACMA mixture was supplemented with 1 mM P_i (trace a), (b) no added P_i, and (c) 1 mM P_i and 2 μM ADP. The proton pumping was started by addition of 100 μM ATP (traces a and b) or 30 μM ATP (trace c), and the 100% fluorescence level was recovered by addition of 0.5 μM nigericine. The corresponding rates of ATP hydrolysis have been measured with Phenol Red (not shown) and were 72, 61, and 33 mM ATP M $Bchl^{-1}$ s^{-1}, respectively.

In the measurements presented so far, the ADP concentration had been modulated in the presence of 1 mM P_i. In the following measurements, the P_i concentration was varied. The ADP concentration resulted from the ADP amount present in the ATP solution (0.7%) and from the ADP produced during hydrolysis, so that in every case a concentration above 1 μM was rapidly generated.

Figure 3 shows ACMA fluorescence traces obtained at 1 mM P_i (curve a) and in the absence of added P_i (curve b). The rates of ATP hydrolysis, measured in parallel in the presence of Phenol Red, were 72 and 61 mM ATP M $Bchl^{-1}$ s^{-1}, respectively. The steady-state fluorescence quenching was severely inhibited in the absence of added P_i, to an extent which was not justified by the 1.2-fold lower rate of ATP hydrolysis. In fact, similarly low-quenching levels could be obtained by limiting the ATP concentration to 30 μM (trace c of Figure 3), thus reducing the hydrolysis rate to 33 mM ATP M $Bchl^{-1}$ s^{-1} (2 μM ADP had also been added to prevent the uncoupled state at the lower ATP concentration). Moreover, particularly striking is the comparison between the kinetics of traces b and c. In the latter case, the low-fluorescence-quenching level is reached slowly, whereas the initial quenching rate of trace b is very similar to the initial quenching rate of trace a and the steady-state quenching level is reached much faster. On the other hand, the kinetics of ATP hydrolysis measured under the corresponding experimental conditions did not deviate significantly from linearity during the time interval of the ACMA assay (not shown). A trace very similar to trace c was obtained by inhibiting ATP hydrolysis with 60 μM ADP (not shown). Therefore, these results indicate that, when the P_i concentration is low enough (no more than 5 μM P_i were produced within the first 2 min of the reaction in the assay of trace b), the ATP synthase is converted into a state that is intrinsically uncoupled, similar to what happens at very low ADP concentrations (see above).

It was of interest to determine the concentration range in which the effect of P_i takes place (Figure 4A). A small increase of steady-state fluorescence quenching was seen already at 10 μM, and it reached saturation in the millimolar range. The pronounced biphasicity of the curves is evident, with a fast phase followed by a slow increase of quenching (e.g., see traces c, d, and e). A plot of the steady-state quenching levels as a function of the P_i concentration is

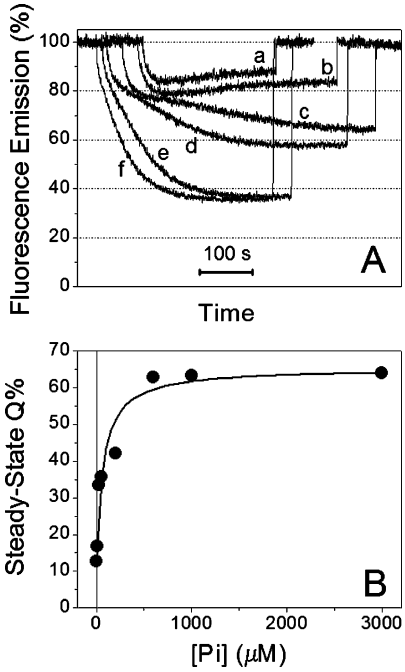

FIGURE 4: ΔpH formation as a function of the P_i concentration. (A) Proton-pumping reaction in the ACMA mixture was started in the spectrofluorometer by addition of 100 μM ATP. (a) no added P_i, (b) 10 μM P_i, (c) 50 μM P_i, (d) 200 μM P_i, (e) 600 μM P_i, and (f) 3 mM P_i. The traces have been translated along the time axis. The corresponding rates of ATP hydrolysis have been measured with Phenol Red (not shown) and varied between 61 (no added P_i) and 74 (3 mM P_i) mM ATP M $Bchl^{-1}$ s^{-1}. (B) Relative steady-state fluorescence quenching, *Q*%, from A and other measurements, was plotted as a function of added P_i. The curve is the best fit to the data of the hyperbolic function $P1 + P2x/(P3 + x)$, with best-fit parameters P1 = 12, P2 = 53, and P3 = 73 μM.

shown in Figure 4B. The data could be fitted with a hyperbolic function, with a half-maximal effect at $[P_i] = 73$ μM. A similar set of measurements, carried out at pH 8.5 (not shown), shifted the half-maximal P_i concentration to 240 μM, suggesting that the monoanionic species may be involved.

The effect of P_i was investigated by also taking oxonol VI as a probe for $\Delta\tilde{\mu}_{H^+}$ formation, similar to what was done for the effect of ADP. To have a good signal/noise ratio with oxonol VI, a higher concentration of Bchl and ATP had to be used, as in Figure 2. Therefore, P_i production by the ATP hydrolysis reaction was not expected to be negligible, and the difference between the assays in the absence and presence of P_i could not be so clear-cut. As a tool for keeping the P_i concentration low during the assay, we have used a combination of PNP and MESG, which can effectively act as a P_i trap (see the Materials and Methods).

Figure 5A compares the absorbance changes upon addition of ATP either in the presence of 1 mM P_i (trace a), in the presence of P_i trap (trace b), or in the absence of both added P_i and P_i trap (curve c). The inhibiting effect of a P_i trap is striking, equally so when both P_i and P_i trap were omitted (curve c); by comparison with curve a and b, the slow increase of oxonol VI response observed in this case can be attributed to a corresponding slow accumulation of P_i because of ATP hydrolysis.

Again it was essential to measure the rates of ATP hydrolysis under experimental conditions as close as possible to those of the Oxonol assays. In the absence of the P_i trap,

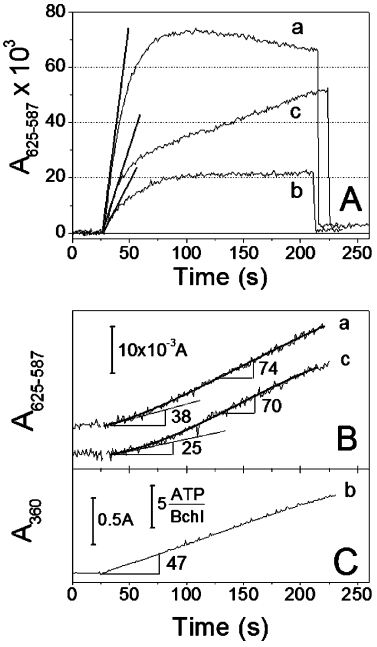

FIGURE 5: $\Delta\varphi$ formation and ATP hydrolysis in the presence of different P_i concentrations. The oxonol mixture was 7.5 μM Bchl. (A) $\Delta\varphi$ formation. The proton-pumping reaction was started in the spectrophotometer by addition of 1 mM ATP, and after 180−200 s, 2 μM valinomycin was added to collapse the $\Delta\varphi$. (a) 1 mM P_i, (b) addition of MESG and PNP, with no added P_i, and (c) no added P_i. The straight lines indicate the initial slope of the traces, which were 3.3, 0.8, and 1.3 mA s^{-1} for traces a, b, and c, respectively. (B) ATP hydrolysis. Oxonol VI was omitted, and Phenol Red was added to the oxonol mixture. ATP hydrolysis was started by addition of 1 mM ATP. The calibration was 3.8 mA/μM H^+ in the absence of added P_i and 3.6 mA/μM H^+ with added P_i. The curve is the best fit to the data of an arbitrary sigmoid function. The numbers at the slope are the rate of ATP hydrolysis in units of mM ATP M Bchl^{-1} s^{-1}. (C) ATP hydrolysis. The oxonol mixture contained MESG, PNP (as for trace b of A), and no oxonol VI. The ATP hydrolysis reaction was started by 1 mM ATP, and the release of P_i was followed at 360 nm. The absorption signal was calibrated in a separated, identical cuvette, by 3-fold addition of 2 μM P_i. The number at the slope is the rate of ATP hydrolysis in units of mM ATP M Bchl^{-1} s^{-1}.

the Phenol Red assay was used as described above (Figure 5B). In the presence of the P_i trap (Figure 5C), an advantage was taken of the fact that the PNP/MESG system can be used for direct monitoring of the rate of P_i formation (see the Materials and Methods). In the absence of the P_i trap, irrespective of the presence of added P_i and as already noticed (see Figure 2B), a biphasic time course of ATP hydrolysis was observed. In this case, the most straightforward analysis can be made by comparing the initial rates of ATP hydrolysis (parts B and C of Figure 5) and oxonol VI absorbance changes (Figure 5A). It can be seen that, in the presence of 1 mM P_i (traces a), the initial rate of ATP hydrolysis is slightly lower than in the presence of the P_i trap, but the initial rate of oxonol VI absorbance change is about 4-fold higher. Analogously, in the absence of both added P_i and P_i trap (traces c), the initial rate of ATP hydrolysis is about 2-fold lower than in the presence of the P_i trap but the initial rate of oxonol VI absorbance change is about 1.6-fold higher. Therefore, the Oxonol assay confirmed what had already been seen in the ACMA assay (see Figure 3), i.e., that not only a low ADP concentration but also a low P_i concentration induces a state of the ATP synthase that is intrinsically uncoupled.

DISCUSSION

The data that we are presenting in this paper indicate that the ATP synthase can also exist in a state or conformation in which it pumps protons much less efficiently than in the usual coupled state. This state is evident when the concentration of either P_i or ADP in the assay is kept very low. The concentrations at which the half-maximal effect was observed were 73 μM for P_i and an estimated 0.5 μM for ADP. Even though the lack of linear response of the probes (see below) does not allow these numbers to be considered as dissociation constants, nevertheless, they indicate an order of magnitude for these parameters. Concentrations of both products high enough to mask the effect are easily reached within a short time in most usual assays. In fact, the phenomenon could be observed in the present paper only under the particular conditions adopted: high level of PK activity for reducing the steady-state ADP concentration, low ATP synthase and ATP concentrations for keeping the concentration of the product P_i at a low level long enough to measure both proton pumping and ATP hydrolysis, or the use of a P_i trap.

As a measure of proton pumping, we have used two different probes, ACMA and oxonol VI, which function according to two different response mechanisms and are also each sensitive to different components of $\Delta\tilde{\mu}_{H^+}$, with ACMA being a probe of ΔpH and oxonol VI being a probe of $\Delta\varphi$. We have obtained the same results irrespective of the probe used, a combination which drastically reduces the possibility of artifacts. The response of ACMA to ΔpH is not linear (e.g., see ref *28*), as much as ΔpH formation is not linear with the rate of proton influx, depending on the inner buffer capacity and membrane permeability of the vesicles. Analogously, the oxonol VI response is not linear with $\Delta\varphi$ (for a review, see ref *34*). However, the lack of linearity cannot explain the data, because a decrease of the probe response corresponded in general to either a similar rate of ATP hydrolysis (Figure 1) or even a higher rate (Figures 2 and 5). Also striking was the time course of the ACMA signal in the absence of P_i, if compared to the time course under conditions expected to decrease proton pumping by decreasing the ATP hydrolysis rate (Figure 3). In the first case, the low steady-state ΔpH was reached abruptly, while it was reached much more slowly when the ATP hydrolysis rate was kept low by lowering the substrate concentration. The comparison indicates that, upon addition of ATP in the absence of P_i, the ATP synthase undergoes a switch from an initial state of efficient proton pumping to a state of reduced efficiency. A similar striking behavior of the time course of probe response can be seen throughout, e.g., see also Figures 1 and 2, where increasing the amounts of PK decrease the steady-state $\Delta\tilde{\mu}_{H^+}$ level but increase the very initial rate of the probe response, again indicating the same type of switch. The initial faster rate of proton pumping in the presence of PK is consistent with the higher activity of the ATP synthase expected when the concentration of inhibitory ADP is decreased.

This sudden transition suggests that, prior to starting the reaction, the enzyme is in the coupled state, changing to the uncoupled state in the course of the reaction, possibly induced

by the buildup of $\Delta\tilde{\mu}_{H^+}$ or by the ATP itself. The residual steady-state $\Delta\tilde{\mu}_{H^+}$, observed at the lowest ADP or P_i concentrations maintained under our experimental conditions, could be due to a heterogeneity in the catalytic state among the ATP synthase population and/or to the fact that the intrinsic uncoupling, which characterizes the catalysis of the low-efficiency state, is not total but rather partial.

According to our data and our interpretation, the uncoupled state is switched back to the coupled state by the binding of both ADP and P_i. It is remarkable that ADP binds at submicromolar concentrations, while ATP (that could bind competitively) is present at millimolar concentrations. This high affinity appears to be 1−2 orders of magnitude higher than that characterizing the binding of the inhibitory ADP under the experimental conditions of the present paper. Interestingly, also the light-induced increase of the ATP hydrolysis activity in *Rb. capsulatus* chromatophores was shown to be inhibited by ADP at submicromolar concentrations (*35*).

The different ADP concentrations, at which intrinsic uncoupling on one side and hydrolysis inhibition on the other side occur, clearly indicate that the binding of ADP on the enzyme takes place at two distinct sites (a high- and a medium-affinity site). The presence of two ADP bound to sites of different affinities ($K_d = 0.1$ and 20 μM, respectively) has been reported for the *Escherichia coli* ATP synthase in which reporter Trp's had been inserted close to the catalytic site (*36*). A model has been advanced in which both ADPs are present simultaneously during the catalytic cycle of hydrolysis. This model has recently obtained strong support in a study on the mechanochemical-coupling mechanism in PS3 F_1 in which rotation and site occupancy by a fluorescent ATP analogue were observed simultaneously (*37*). It appears likely that the double effect of ADP observed by us is related to the occupancy of these two sites and that the depletion of ADP from the external medium, caused by PEP and PK additions, deprives of ADP not only the medium- but also the high-affinity site, thereby triggering a different functional state.

If indeed ADP and P_i bind to a (high-affinity) catalytic site, the enzyme must have a way to release both ligands after they have bound, unless the rotational catalysis is inhibited. The most efficient way to accomplish this task, i.e., to change dramatically their binding affinity, is probably to transform them into ATP, which would then be released as such. Should this hypothesis be correct, ADP and P_i would necessarily bind to the same catalytic site. Interesting enough, low levels of ATP synthesis from medium ADP and P_i, inhibited by increasing PK, are invariably found during ATP hydrolysis in the presence of a $\Delta\tilde{\mu}_{H^+}$ (so-called "ATP−P_i exchange") even at very high ATP/ADP ratios (*23*, *38*, *39*).

To our knowledge, the occurrence during ATP hydrolysis of an intrinsically uncoupled state of the unmodified, wild-type ATP synthase has never been reported before. The existence of a state of high proton conductivity of the ATP synthase in the absence of substrates has been observed for a long time in chloroplasts (see the Introduction) and more recently in *Rb. capsulatus* chromatophores as well (*21*). The high-conductivity state could be measured following a train of actinic flashes in the absence of phosphorylation substrates and was switched back to a low-conductivity state by binding of ADP and P_i at micromolar concentrations (*20*). It remains to be investigated whether these phenomena are different aspects of the same basic feature or not. More recently, a high-conductivity state of the chloroplast ATP synthase has been measured in intact leaves (*40*). These authors hypothesized that this state could serve as a physiological way of regulating the extent of $\Delta\tilde{\mu}_{H^+}$ in chloroplasts and that it could be modulated by P_i.

Whether this phenomenon is a common feature for all ATP synthases, as we think likely, or rather it is specific of these photosynthetic prokaryotic membranes, is a matter for further investigation. It is an intriguing possibility that the uncoupled state of ATP synthase, which we are reporting, might have a regulatory role in energy-transducing membranes, similar to the regulatory role hypothesized for the intrinsic uncoupling observed in other chemiosmotic enzymes, such as cytochrome oxidase (for a review, see ref *41*), V-ATPases (*42*−*44*), and Ca-ATPases (for a review, see ref *45*). While the ADP concentration in the cytoplasm is unlikely to ever fall below 1 μM, the P_i concentration may well vary in the tens to hundreds of micromolar range.

An obvious question is which structural features of the ATP synthase could be involved in the transition between the coupled and the uncoupled states of the enzyme. Mutagenetic and structural studies, mainly in *E. coli*, have frequently implicated the ϵ subunit as one key structural feature in the coupling mechanism, a role which appears to be highly plausible in view of its positioning within the complex, its structure, and its functional links to both events at the catalytic sites in F_1 and at the proton-binding sites in F_0 (*9*, *46*, and references therein). The recent findings of at least two very different conformational states of the ϵ subunit within the complex (*47*−*50*), in which the C-terminal α-helix hairpin of the ϵ subunit is either bent toward F_0 ("down-state") or is extended toward F_1 ("up-state"), make it plausible that a physiological modulation of coupling by this subunit might exist.

From trypsinization sensitivity (*51*) and fluorescence studies (*52*), it has been shown that a change in the ϵ conformation is brought about by P_i binding with high affinity (50−250 μM) to a site suggested by the data to be catalytic. On the basis of a protein-fusion study, Cipriano et al. (*10*) have argued that one function of the ϵ subunit in the ATP synthase is to inhibit an uncoupled ATP hydrolysis reaction, in particular the C terminus of ϵ in the up-state would prevent uncoupling. It is a recent finding (*49*, *50*) that the transition of the ϵ subunit from the down- to the up-state is associated to a functional switch from an enzyme favoring ATP hydrolysis to one more active in ATP synthesis.

It is particularly tempting to speculate that the down and the up conformations correspond to the uncoupled and the coupled states referred to in the present paper. Indeed, as noted in Cipriano et al. (*10*), the down conformation, immobilized by site-specific −S−S− bonds in Tsunoda et al. (*49*), appears to be at least in part uncoupled. Also, recent evidence indicate that, in the absence of nucleotides, the ATP synthase is in the up-state and that ATP induced the transition to the down-state, whereas ADP counteracted this effect; moreover, $\Delta\tilde{\mu}_{H^+}$ stabilized the up-state (*50*).

The uncoupled state (ϵ down-state in our hypothesis), being much less efficient in energy transduction and therefore presumably in ATP synthesis, would then correspond to the

so-called "hydrolase" form (*49*, *51*). Analogously, the coupled state (ϵ up-state), being mostly inhibited in its hydrolytic activity because of the back pressure of $\Delta\tilde{\mu}_{H^+}$, would correspond to the "synthase" form. In contrast with this hypothesis, the chloroplast ATP synthase has been shown to catalyze ATP synthesis at a similar level with both the native and C-terminal truncated ϵ subunit (*52*, *53*). However, because the enzyme with the truncated ϵ subunit was less inhibited in the hydrolysis direction, it should have been more active during synthesis as well, indicating that it could have a less efficient synthesis.

Within the proposed framework, it might be of interest to hypothesize a possible mechanism of uncoupling related to the ϵ subunit being in the down-state. Some possibilities are, e.g., that the surface of interaction between the γ/ϵ and the c-subunits complex is changed in the down-state so that it is weakened and a slip between these two rotor components is more likely, or that a slip takes place between the c oligomer and the a subunit. Alternatively, a slip might take place between the $\alpha_3\beta_3$ barrel and the γ subunit. The recent finding of Suzuki et al. (*50*), indicating that the C-terminal helix of the ϵ subunit, in the up-state, is hosted within the $\alpha_3\beta_3$ barrel as a third helix together with the two coiled helices of the γ subunit, might suggest that placement of the third helix outside the $\alpha_3\beta_3$ barrel could weaken the structural interactions between the rotor and the catalytic domains, favoring slipping.

ACKNOWLEDGMENT

We thank G. Venturoli for critical reading of the paper.

REFERENCES

1. Boyer, P. D. (1997) The ATP synthase—A splendid molecular machine, *Annu. Rev. Biochem. 66*, 717−749.
2. Fillingame, R. H., Jiang, W., and Dmitriev, O. Y. (2000) Coupling H^+ transport to rotary catalysis in F-type ATP synthases: Structure and organization of the transmembrane rotary motor, *J. Exp. Biol. 203*, 9−17.
3. Yoshida, M., Muneyuki, E., and Hisabori, T. (2001) ATP synthase—A marvellous rotary engine of the cell, *Nat. Rev. Mol. Cell. Biol. 2*, 669−677.
4. Capaldi, R. A., and Aggeler, R. (2002) Mechanism of the F_1F_0-type ATP synthase, a biological rotary motor, *Trends Biochem. Sci. 27*, 154−160.
5. Abrahams, J. P., Leslie, A. G., Lutter, R., and Walker, J. E. (1994) Structure at 2.8 Å resolution of F_1-ATPase from bovine heart mitochondria, *Nature 370*, 621−628.
6. Wang, H., and Oster, G. (1998) Energy transduction in the F_1 motor of ATP synthase, *Nature 396*, 279−282.
7. Junge, W., Panke, O., Cherepanov, D. A., Gumbiowski, K., Muller, M., and Engelbrecht, S. (2001) Inter-subunit rotation and elastic power transmission in F_0F_1-ATPase, *FEBS Lett. 504*, 152−160.
8. Gardner, J. L., and Cain, B. D. (1999) Amino acid substitutions in the a subunit affect the ϵ subunit of F_1F_0 ATP synthase from *Escherichia coli*, *Arch. Biochem. Biophys. 361*, 302−308.
9. Peskova, Y. B., and Nakamoto, R. K. (2000) Catalytic control and coupling efficiency of the *Escherichia coli* F_0F_1 ATP synthase: Influence of the F_0 sector and ϵ subunit on the catalytic transition state, *Biochemistry 39*, 11830−11836.
10. Cipriano, D. J., Bi, Y., and Dunn, S. D. (2002) Genetic fusions of globular proteins to the ϵ subunit of the *Escherichia coli* ATP synthase: Implications for in vivo rotational catalysis and ϵ subunit function, *J. Biol. Chem. 277*, 16782−16790.
11. Pick, U., and Weiss, M. (1988) A light-dependent dicyclohexylcarbodiimide-sensitive Ca-ATPase activity in chloroplasts which is not coupled to proton translocation, *Eur. J. Biochem. 173*, 623−628.
12. Casadio, R., and Melandri, B. A. (1996) CaATP inhibition of the MgATP-dependent proton pump (H^+-ATPase) in bacterial photosynthtic membranes with a mechanism of alternate substrate inhibition, *J. Bioinorg. Chem. 1*, 284−291.
13. Cappellini, P., Turina, P., Fregni, V., and Melandri, B. A. (1997) Sulfite stimulates the ATP hydrolysis activity of but not proton translocation by the ATP synthase of *Rhodobacter capsulatus* and interferes with its activation by $\Delta\mu_{H^+}$, *Eur. J. Biochem. 248*, 496−506.
14. Van Walraven, H. S., Scholts, M. J., Lill, H., Matthijs, H. C., Dilley, R. A., and Kraayenhof, R. (2002) Introduction of a carboxyl group in the loop of the F_0 c-subunit affects the H^+/ATP coupling ratio of the ATP synthase from Synechocystis 6803, *J. Bioenerg. Biomembr. 34*, 445−454.
15. Schemidt, R. A, Qu, J., Williams, J. R., and Brusilow, W. S. (1998) Effects of carbon source on expression of F_0 genes and on the stoichiometry of the c subunit in the F_1F_0 ATPase of *Escherichia coli*, *J. Bacteriol. 180*, 3205−3208.
16. Olsson, K., Keis, S., Morgan, H. W., Dimroth, P., and Cook, G. M. (2003) Bioenergetic properties of the thermoalkaliphilic *Bacillus* sp. strain TA2.A1, *J. Bacteriol. 185*, 461−465.
17. McCarty, R. E., Fuhrman, J. S., and Tsuchiya, Y. (1971) Effects of adenine nucleotides on hydrogen-ion transport in chloroplasts, *Proc. Natl. Acad. Sci. U.S.A. 68*, 2522−2526.
18. Gräber, P., Burmeister, M., and Hortsch, M. (1981) Regulation of the membrane permeability of the spinach chloroplasts by binding of adenine nucleotides, *FEBS Lett. 136*, 25−31.
19. Evron, Y., and Avron, M. (1990) Characterization of an alkaline pH-dependent proton "slip" in the ATP synthase of lettuce thylakoids, *Biochim. Biophys. Acta 1019*, 115−120.
20. Groth, G., and Junge, W. (1993) Proton slip of the chloroplast ATPase: Its nucleotide dependence, energetic threshold, and relation to an alternating site mechanism of catalysis, *Biochemistry 32*, 8103−8111.
21. Feniouk, B. A., Cherepanov, D. A., Junge, W., and Mulkidjanian, A. Y. (1999) ATP-synthase of *Rhodobacter capsulatus*: Coupling of proton flow through F_0 to reactions in F_1 under the ATP synthesis and slip conditions, *FEBS Lett. 445*, 409−414.
22. Borghese, R., Crimi, M., Fava, L., and Melandri B. A. (1998) The ATP synthase *atpHAGDC* (F_1) operon from *Rhodobacter capsulatus*, *J. Bacteriol. 180*, 416−421.
23. Baccarini-Melandri, A., and Melandri, B. A. (1971) Partial resolution of phosphorylating system of *Rps. capsulata*, *Methods Enzymol. 23*, 556−561.
24. Clayton, R. K. (1963) Toward the isolation of a photochemical reaction center in *Rhodopseudomonas sphaeroides*, *Biochim. Biophys. Acta 75*, 312−323.
25. Nishimura, M., Ito, T., and Chance, B. (1962) Studies on bacterial photophosphorylation. III. A sensitive and rapid method of determination of photophosphorylation, *Biochim. Biophys. Acta 59*, 177−182.
26. Lanzetta, P. A., Alvarez, L. J., Reinach, P. S., and Candia, O. A. (1979) An improved assay for nanomole amounts of inorganic phosphate, *Anal. Biochem. 100*, 95−97.
27. Webb, M. R. (1992) A continuous spectrophotometric assay for inorganic phosphate and for measuring phosphate release kinetics in biological systems, *Proc. Natl. Acad. Sci. U.S.A. 89*, 4884−4488.
28. Casadio, R., and Melandri, B. A. (1985) Calibration of the response of 9-amino acridine fluorescence to transmembrane pH differences in bacterial chromatophores, *Arch. Biochem. Biophys. 238*, 219−228.
29. Jackson, J. B., and Crofts, A. R. (1971) The kinetics of light induced carotenoid changes in *Rhodopseudomonas spheroides* and their relation to electrical field generation across the chromatophore membrane, *Eur. J. Biochem. 18*, 120−130.
30. Bashford, C. L., Chance, B., and Prince, R. C. (1979) Oxonol dyes as monitors of membrane potential. Their behavior in photosynthetic bacteria, *Biochim. Biophys. Acta 545*, 46−57.
31. Zannoni, D., Melandri, B. A., and Baccarini-Melandri, A. (1976) Energy transduction in photosynthetic bacteria. X. Composition and function of the branched oxidase system in wild type and respiration deficient mutants of *Rhodopseudomonas capsulata*, *Biochim. Biophys. Acta 423*, 413−430.
32. McQuate, J. T., and Utter, M. F. (1959). Equilibrium and kinetic studies of the pyruvic kinase reaction, *J. Biol. Chem. 234*, 2151−2157.
33. Turina, P., Rumberg, B., Melandri, B. A., and Gräber, P. (1992) Activation of the H^+-ATP synthase in the photosynthetic bacterium *Rhodobacter capsulatus*, *J. Biol. Chem. 267*, 11057−11063.

34. Smith, J. C. (1990) Potential-sensitive molecular probes in membranes of bioenergetic relevance, *Biochim. Biophys. Acta 1016*, 1−28.
35. Melandri, B. A., Baccarini-Melandri, A., and Fabbri, E. (1972) Energy transduction in photosynthetic bacteria. IV. Light-dependent ATPase in photosynthetic membranes from *Rhodopseudomonas capsulata*, *Biochim. Biophys. Acta 275*, 383−394.
36. Weber, J., and Senior, A. E. (2000) ATP synthase: What we know about ATP hydrolysis and what we do not know about ATP synthesis, *Biochim. Biophys. Acta 1458*, 300−309.
37. Nishizaka, T., Oiwa, K., Noji, H., Kimura, S., Muneyuki, E., Yoshida, M., and Kinosita, K., Jr. (2004) Chemomechanical coupling in F_1-ATPase revealed by simultaneous observation of nucleotide kinetics and rotation, *Nat. Struct. Mol. Biol. 11*, 142−148.
38. Carmeli, C., Lifschitz, Y. (1969) The requirements of adenosine diphosphate for light-triggered ATPase and ATP−P_i exchange reactions in chloroplasts, *FEBS Lett. 5*, 227−230.
39. Davenport, J. W., and McCarty, R. E. (1981) Quantitative aspects of adenosine triphosphate-driven proton translocation in spinach chloroplast thylakoids, *J. Biol. Chem. 256*, 8947−8954.
40. Kanazawa, A., and Kramer, D. M. (2002) In vivo modulation of nonphotochemical exciton quenching (NPQ) by regulation of the chloroplast ATP synthase, *Proc. Natl. Acad. Sci. U.S.A. 99*, 12789−12794.
41. Kadenbach, B. (2003) Intrinsic and extrinsic uncoupling of oxidative phosphorylation, *Biochim. Biophys. Acta 1604*, 77−94.
42. Moriyama, Y., and Nelson, N. (1988) The vacuolar H^+-ATPase, a proton pump controlled by a slip, *Prog. Clin. Biol. Res. 273*, 387−394.
43. Davies, J. M., Hunt, I., and Sanders, D. (1994) Vacuolar H^+-pumping ATPase variable transport coupling ratio controlled by pH, *Proc. Natl. Acad. Sci. U.S.A. 91*, 8547−8551.
44. Müller, M. L., Jensen, M., and Taiz, L. (1999) The vacuolar H^+-ATPase of lemon fruits is regulated by variable H^+/ATP coupling and slip, *J. Biol. Chem. 274*, 10706−10716.
45. Berman, M. C. (2001) Slippage and uncoupling in P-type cation pumps; implications for energy transduction mechanisms and regulation of metabolism, *Biochim. Biophys. Acta 1513*, 95−121.
46. Dunn, S. D. (1995) A barrel in the stalk, *Nat. Struct. Biol. 2*, 915−918.
47. Gibbons, C., Montgomery, M. G., Leslie, A. G., and Walker, J. E. (2000) The structure of the central stalk in bovine F_1-ATPase at 2.4 Å resolution, *Nat. Struct. Biol. 7*, 1055−1061.
48. Rodgers, A. J., and Wilce, M. C. (2000) Structure of the $\gamma-\epsilon$ complex of ATP synthase, *Nat. Struct. Biol. 11*, 1051−1054.
49. Tsunoda, S. P., Rodgers, A. J., Aggeler, R., Wilce, M. C., Yoshida, M., and Capaldi, R. A. (2001) Large conformational changes of the ϵ subunit in the bacterial F_1F_0 ATP synthase provide a ratchet action to regulate this rotary motor enzyme, *Proc. Natl. Acad. Sci. U.S.A. 98*, 6560−6564.
50. Suzuki, T., Murakami, T., Iino, R., Suzuki, J., Ono, S., Shirakihara, Y., and Yoshida, M. (2003) F_0F_1-ATPase/synthase is geared to the synthesis mode by conformational rearrangement of ϵ subunit in response to proton motive force and ADP/ATP balance, *J. Biol. Chem. 278*, 46840−46846.
51. Mendel-Hartvig, J., and Capaldi, R. A. (1991) Catalytic site nucleotide and inorganic phosphate dependence of the conformation of the ϵ subunit in *Escherichia coli* adenosinetriphosphatase, *Biochemistry 30*, 1278−1284.
52. Turina, P. (2000) Structural changes during ATP hydrolysis activity of the ATP synthase from *Escherichia coli* as revealed by fluorescent probes, *J. Bioenerg. Biomembr. 32*, 373−381.
53. Vinogradov, A. D. (2000) Steady-state and pre-steady-state kinetics of the mitochondrial F_1F_0 ATPase: Is ATP synthase a reversible molecular machine? *J. Exp. Biol. 203*, 41−49.
54. Nowak, K. F., Tabidze, V., and McCarty, R. E. (2002) The C-terminal domain of the ϵ subunit of the chloroplast ATP synthase is not required for ATP synthesis, *Biochemistry 41*, 15130−15234.
55. Nowak, K. F., and McCarty, R. E. (2004) Regulatory role of the C-terminus of the ϵ subunit from the chloroplast ATP synthase, *Biochemistry 43*, 3273−3279.

BI048975+